30th Annual International IEEE EMBS Conference
Vancouver, British Columbia, Canada, August 20-24, 2008

Compressed Sensing Parallel Magnetic Resonance Imaging

Jim X. Ji, Chen Zhao, and Tao Lang
Department of Electrical and Computer Engineering, Texas A&M University

Abstract—**Both parallel Magnetic Resonance Imaging (pMRI) and Compressed Sensing (CS) can significantly reduce imaging time in MRI, the former by utilizing multiple channel receivers and the latter by utilizing the sparsity of MR images in a transformed domain. In this work, pMRI and CS are integrated to take advantages of the sensitivity information from multiple coils and sparsity characteristics of MR images. Specifically, CS is used as a regularization method for the inverse problem raised by pMRI based on the L1 norm and a Total Variation (TV) term. We test the new method with a set of 8-channel, *in-vivo* brain MRI data at reduction factors from 2 to 8. Reconstruction results show that the proposed method outperforms several other regularized parallel MRI reconstruction such as the truncated Singular Value Decomposition (SVD) and Tikhonov regularization methods, in terms of residual artifacts and SNR, especially at reduction factors larger than 4.**

Keywords—**Parallel MRI, compressed sensing, regularization, imaging reconstruction**

I. INTRODUCTION

Magnetic resonance imaging (MRI) is a relative slow imaging modality as compared with X-ray CT, ultrasound imaging, and optical imaging. Parallel MRI (pMRI) is an effective way to reduce the imaging time by using multiple-channel receiver and array coils to acquire data in parallel. Typically, the k-space is covered with reduced number of data points to save time and a special reconstruction is used to form the image. In the SENSE method, the image is reconstructed from partially collected data together with the channel sensitivity information using a linear system framework. However, directly solving the inverse problem raised by pMRI can be unstable due to poor numerical conditions and poorly estimated channel sensitivity information. To address this problem, many regularization methods have been proposed. The Singular Value Decomposition (SVD) method simply sets up a threshold to the eigenvalues and discards the eigenvalues below the threshold, as illustrated in the SPACE-RIP (Sensitivity Profiles from an Array of Coils for Encoding and Reconstruction in Parallel) method [1]. Another popular regularization method, Tikhonov regularization, tries to improve the conditioning by using a regularization matrix and adding a regularization parameter to diagonal terms of the system equation [2,3,4,5]. Both methods are based on L2 norm and they assume the minimal image energy prior.

The Compressed Sensing (CS) method was first introduced in the literature of Information Theory and Approximation Theory [6,7]. The basic idea is that a signal can be reconstructed from its spectrum, even the spectrum is sampled at a rate below the Nyquist criterion (undersampling), if the following conditions hold: First, the signal must have a sparse representation in a transformed domain (i.e., it must be compressible by some transform coding scheme). Second, the aliasing artifacts in a linear reconstruction caused by undersampling must be incoherent (noise-like) in the sparsifying transform domain. Under these conditions, the signal can be reconstructed using a non-linear method which enforces both sparsity representation of the signal and consistency of the reconstruction with the acquired samples. Lustig and his colleagues have successfully implemented the CS method into MRI recently [8]. In their work, CS was applied to single-channel MR imaging for angiography, coronary imaging, and brain imaging with promising results. For example, an undersampling factor of 2.4 was achieved for brain images without significant loss of reconstruction quality.

In this work, we treat CS as a regularization method for pMRI, which can take advantages of the sensitivity information from muliple coils and sparsity information of MR images.

II. METHODOLOGY

The forward imaging equation in pMRI can be formulated as a linear problem as shown in [1]. Without loss of generality, assuming that the k-space data is sampled on a 2-D Cartesian grid (x, y) and the frequency encoding direction x has been resolved using inverse FFT. For each x, let n_a denote the undersampled data points per channel, n_c denote the total number of receiver channels, $W(y)$ denote the channel sensitivity function, G_y^g denote the phase encoding gradient applied during the g^{th} acquisition, τ denote the pulse width of the phase encoding gradient G_y^g, and N denote the image size along the phase encoding direction. Then the imaging equation at this specific frequency encoding position can be formed as:

$$S = W\rho \tag{1}$$

where S is the $(n_a \times n_c) \times 1$ observation vector of the multi-channel k-space data, W is a $(n_a \times n_c) \times N$ forward matrix

which incorporates the gradient-induced and sensitivity encoding information, and ρ is a $N \times 1$ desired image vector. Specifically,

$$\begin{pmatrix} S_1(1) \\ S_1(2) \\ \vdots \\ S_1(n_a) \\ \vdots \\ S_{n_c}(1) \\ S_{n_c}(2) \\ \vdots \\ S_{n_c}(n_a) \end{pmatrix} = \begin{pmatrix} W_1(1)e^{i\gamma(G_y^1 1\tau)} & \cdots & W_1(N)e^{i\gamma(G_y^1 N\tau)} \\ W_1(1)e^{i\gamma(G_y^2 1\tau)} & \cdots & W_1(N)e^{i\gamma(G_y^2 N\tau)} \\ \vdots & \cdots & \vdots \\ W_1(1)e^{i\gamma(G_y^{n_a} 1\tau)} & \cdots & W_1(N)e^{i\gamma(G_y^{n_a} N\tau)} \\ \vdots & \cdots & \vdots \\ W_{n_c}(1)e^{i\gamma(G_y^1 1\tau)} & \cdots & W_{n_c}(N)e^{i\gamma(G_y^1 N\tau)} \\ W_{n_c}(1)e^{i\gamma(G_y^2 1\tau)} & \cdots & W_{n_c}(N)e^{i\gamma(G_y^2 1\tau)} \\ \vdots & \cdots & \vdots \\ W_{n_c}(1)e^{i\gamma(G_y^1 1\tau)} & \cdots & W_{n_c}(N)e^{i\gamma(G_y^1 N\tau)} \end{pmatrix} \cdot \begin{pmatrix} \rho(1) \\ \rho(2) \\ \rho(3) \\ \vdots \\ \rho(N) \end{pmatrix} \quad (2)$$

Forming and solving the equation for each frequency encoding position will yield a 2-D image. In the conventional image-space reconstruction, ρ is solved using the minimal least-squares solution:

$$\hat{\rho} = (W^H \psi^{-1} W)^{-1} W^H \psi^{-1} S \quad (3)$$

where ψ is the covariance matrix of the observation noise. However, this method tends to amplify noise when matrix W is poorly conditioned, i.e., with large condition number (i.e. the ratio of the largest eigenvalue to the smallest eigenvalue). Thus the estimated image vector $\hat{\rho}$ may contain large artifacts and has low SNR.

Various regularization methods have been proposed to address this problem. In [1], the solution to Eq. (1) is obtained using the SVD method:

$$\hat{\rho} = \sum_i \frac{1}{\lambda_i} v_i u_i^H \rho \quad (4)$$

with v_i and u_i being the left and right singular vectors of W in Eq. (1) respectively, corresponding to the singular value λ_i. The λ_i less than 5% of the maximum eigenvalue are removed to overcome the ill-conditioning problem. This can effectively reduce the noise amplification. In [4], the Tikhonov regularization method was used, i.e.,

$$\hat{\rho} = \arg\min \| W\rho - S \|_2^2 + \beta \| \Gamma\rho \|_2^2 \quad (5)$$

where $\| \bullet \|_2$ denotes the L_2 norm, β is the regularization parameter and Γ is called the Tikhonov matrix which can be as simple as an identity matrix or other operators on the image. Then, the solution is given by:

$$\hat{\rho} = (W^H W + \beta \Gamma^H \Gamma)^{-1} W^H S \quad (6)$$

Note that larger β can further suppress noise amplification but tend to oversmooth the reconstructed image. Typically β is set by experimental trials or the L-curve method to strike a balance between the noise amplification and the smoothness of the reconstructed images [3].

Using the CS principle, the proposed method acquires undersampled k-space in a semi-random fashion along the phase encoding direction, and it solves Eq. (1) by

$$\| W\rho - S \|_2^2 + \lambda_1 \| F\rho \|_1 + \lambda_2 TV(\rho) \quad (7)$$

Here, $\| \bullet \|_1$ represents the L-1 norm defined as $\| x \|_1 = \sum | x_i |$. $TV(\rho)$ is the Total Variation defined as $TV(\rho) = \int | \nabla\rho | d\rho$, where ∇ is the spatial gradient operator.

The *TV* regularization method is a widely-used objective in image processing to impose some level of continuity on the image [9,10]. F denotes the sparse transform matrix (e.g. the wavelet transform) to compress the signal into a "sparse" representation. λ_1 and λ_2 are the regularization parameters. Note that the first term enforces data consistency in the L_2 sense. Among all solutions which are consistent with the acquired data, the new method will find a solution which is sparse both in the transformed domain and the finite-differences domain. The optimization process is achieved using a non-linear conjugate gradient with fast backtracking method [8]. All algorithms were implemented in Matlab based on the sparseMRI and PULSAR tools [11, 12].

In practice, there are three associated issues. First, the undersampling pattern for the k-space data: we choose a semi-random pattern which is dense in the k-space center and sparse in the outer k-space as discussed in [1,13]. This is because most of the energy of MR signals is concentrated in the center portion of k-space. The patterns for different Rs are shown in Fig. 1. Second, the regularization parameters: currently we don not have any rigorous mathematical algorithms or criteria to select them. Instead, the regularization parameters are chosen using an modified L-curve method. That is, λ_2 in Eq. (7) is set to be zero temporally and the approximately proper value of λ_1 is determined using L-curve. Then λ_1 is set to zero and λ_2 is determined in a similar fashion. It was found that too smal *regularization parameters* cause noise amplification and degradation in reconstruction results. On the other hand, too larger *regularization parameters* cause resolution loss and oversmoothing. This is as expected since total variance could be viewed as another sparse transform. The final step is to tune both λ_1 and λ_2 simultaneously to find a combination around the values previously determined which reduces noise amplifications and aliasing artifacts with no apparent oversmoothness. Third, the proper sparse transform: in this work, F is chosen to be the Daubechies Wavelets Transform with level four, since it can render a relative high compression rate of brain images we tested. However, other sparsifying transformations may perform better if it can be identified.

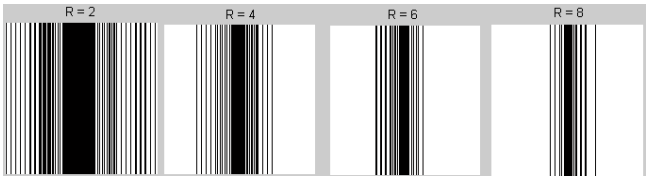

Figure 1. Variable density k-space undersampling patterns for different reduction factors. In 2-D imaging, the undersampling is along the horizontal (phase encoding) direction.

III. RESULTS

To test the algorithm, a set of brain data of a healthy volunteer with 128 encodings was acquired on a 1.5 T scanner using an 8-channel head array coil and fast spin-echo sequence. A separate data set acquired using a fast gradient-echo sequence is used for coil sensitivity calibration. The phase encodings are retrospectively decimated according to the patterns in Figure 1 to simulated the undersampling with R from 2-8 along the phase encoding direction. Reconstructions are performed using the three regularization methods: the truncated SVD method with a cutoff threshold of 5% of the maximum eigenvalue; the Tikhonov regularization with β = 0.4 based on experimental trials and Γ being the identity matrix as discussed in the previous section; and the proposed method with $\lambda_1 = 0.07$ and $\lambda_2 = 0.02$.

Figure 2 shows the reconstructions by the three different methods. As shown, truncated SVD reconstruction shows significant aliasing artifacts (see arrows in first row for R = 6 and 8). The Tikhonov method can smooth the images to some extent but is still affected by artifacts and noise. In contrast, it seems that in this example the new method outperforms the other two at all reduction factors. It suppresses residual aliasing artifacts as well as noise. This is more apparent with increased R. The resolution loss is not clear here, however, with large regularization parameters of λ_1 and λ_2, the oversmoothness and resolution loss are more obvious (not shown).

Figure 3 shows the SNR of different reconstructions. The SNR is calculated based on a signal region **S** and a noise region **N** base on the following formula:

$$SNR = 20\log_{10}\frac{\sum_{i=1}^{P}|I_i|/P}{\sqrt{\sum_{j=1}^{Q}(n_j-\bar{n})^2/Q}}$$

where P is the total number of pixels in **S**, Q is the total number of pixels in **N**, and $\bar{n}$ is the average intensity of noise pixels. As expected, all methods experience a SNR loss with increased R. At R=2, SNRs of the three methods are all close 32 dB, which indicates that the three method have similar effects for the regularization. When R goes higher, the SNR gain from the CS method become more obvious, with a 4 dB increase at R = 8 compared to the SVD method.

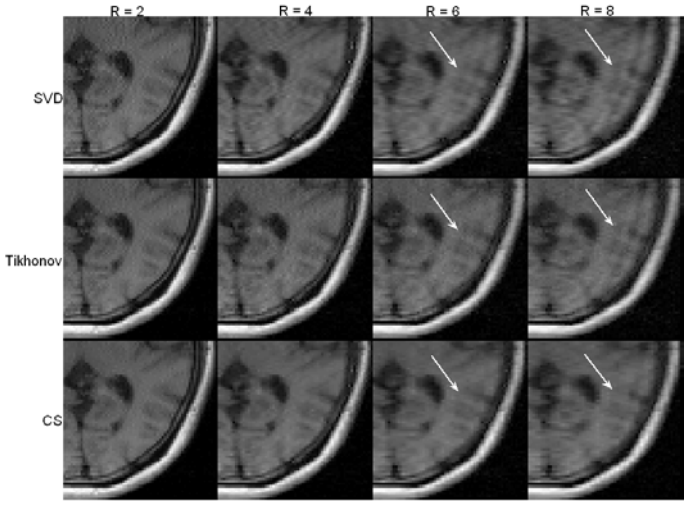

Figure 2. Reconstructions with different methods at different Rs. Only a portion of the image is shown for better visualization The aliasing artifacts in SVD and Tikhonov methods are detectable (white arrows).

The mean square errors (MSE) of reconstructed images with respect to the ground truth are shown in Fig. 4. It shows that the proposed method yields images with least MSE.

Figure 5 is a plot of the convergence behavior of the proposed CS pMRI reconstruction for the experiment described and with R=8. The vertical axis shows the total cost function including the data fitting error and the two regularization terms. Note in this case the reconstruction algorithm converged after about 120 iterations. We also compute the data fitting error (the first term in Eq. (7)), it went down in the beginning but then started to increase after about 25 iterations. This phenomenon (not shown due to space limit) seems to suggest that in order to get a reasonable reconstruction from the proposed method, the iterations should also be monitored or judicially chosen.

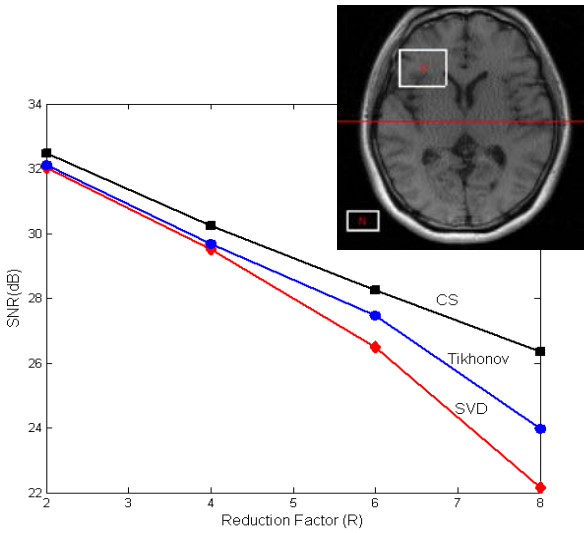

Figure 3. SNRs the mages reconstructed using the three methods

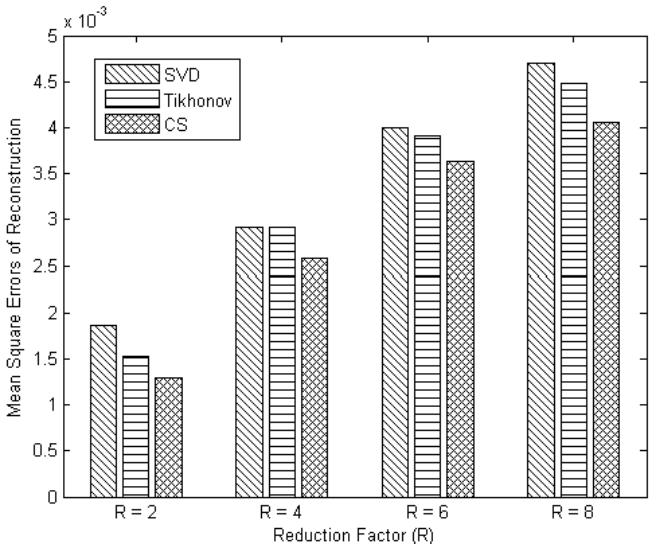

Figure 4. Mean Square Errors (MSE) of reconstructed images with respect to the ground truth. The three methods at four different reduction factors are compared.

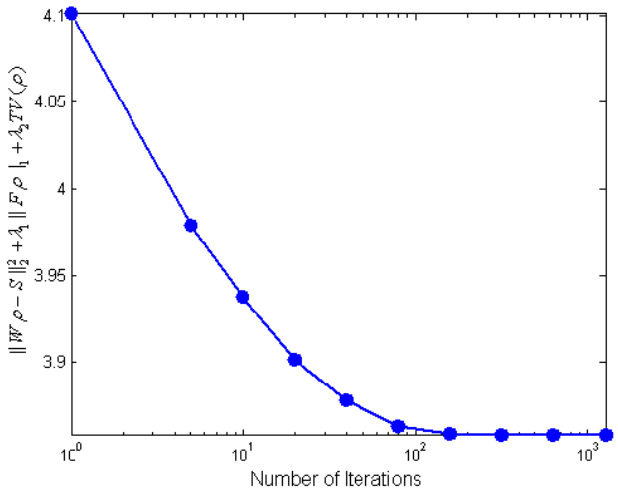

Figure 5. Convergence of the proposed reconstruction method in the brain imaging experiment. The vertical axis represents the whole cost function defined in Eq. (7).

IV. DISCUSSIONS

Incorporating the sparsity of MR images in the regularization method can further improve reconstruction in parallel MRI compared to traditional SVD and Tikhonov regularization methods. The propsed method has the potential to reduced the residual aliasing artifacts and noise but it also tends to oversmooth images and cause resolution degradation if regularization parameters are not set properly.

There are several issues to be addressed in the future work. For example, automatic and optimal selection of the regularization parameters and selection of sparsifying transforms. In addition, the data sampling pattern is set to be densely in the center and sparsely in the outer, which may not be the best choice either. Thus, how to individually and jointly optimize the regularization parameters, the sparsifying transform, and undersampling pattern to improve reconstruction results is a challenge. The proposed method needs to be further developed and tested to establish and investigate its utility for clinical applications.

REFERENCES

[1] Kyriakos WE, Panych LP, Kacher DF, Westin CF, Bao SM, Mulkern RV, Jolesz FA. Sensitivity profiles from an array of coils for encoding and reconstruction in parallel (SPACE RIP). Magn Reson Med 2000; 44, pp. 301308.

[2] Clayton DB, Skare S, Golub GH, Modarresi M, Bammer R, Augmented SENSE reconstruction by an improved regularization approach. ISMRM, Miami, Florida, USA, 2005. p. 2438.

[3] Lin FH, Kwong KK, Belliveau JW, Wald LL. Parallel imaging reconstruction using automatic regularization. Magn Reson Med 2004; Vol. 51 (3), pp. 559-567.

[4] Linag ZP, Bammer R, Ji J, Pelc NJ, Glover GH. Improved image reconstruction from sensitivity-encoded data by wavelet denoising and Tikhonov regularization. IEEE Intl. Sys. Biomed. Imaging, 2002; pp.493-496.

[5] Lin FH, Wang FN, Ahlfors SP, Hamalainen MS, Belliveau JW. Parallel MRI reconstruction using variance partitioning regularization. Mag. Reson. Med.2007; vol 58, pp. 735-744.

[6] Cand`es E, Romberg J, Tao T. Robust uncertainty principles: Exact signal reconstruction from highly incomplete frequency information. IEEE Transactions on Information Theory 2006; vol. 52, pp. 489–509.

[7] Donoho DL. Compressed sensing. IEEE Transactions on Information Theory, 2006; vol. 52, pp. 1289–1306.

[8] Lustig M, Donoho DL and Pauly JM. Sparse MRI: The application of compressed sensing for rapid MR imaging. Magnetic Resonance in Medicine, 2007; 58(6):1182-1195.

[9] Rudin L, Osher S, Fatemi E. Non-linear total variation noise removal algorithm. Phys. D 1992; 60:259–268.

[10] Tsaig Y, Donoho DL. Extensions of compressed sensing. Signal Processing 2006; 86:533–548.

[11] http://www.stanford.edu/~mlustig/SparseMRI.html.

[12] Ji JX, Son JB and Rane SD. PULSAR: A MATLAB toolbox for parallel magnetic resonance imaging using array coils and multiple channel receivers. Concepts in Magnetic Resonance Part B, Magnetic Resonance Engineering, 2007;vol. 31B(1), pp.~24-46.

[13] Haldar JP, Hernando D, Sutton BP, and Liang ZP, Data acquisition considerations for compressed sensing in MRI. Proc. 15 ISMRM, 2007, p. 829, Berlin, Germany.